

Early-Holocene Paleo-Tropical Cyclone Activity Inferred from a Sedimentary Sequence in South Yellow Sea, East Asia

Geng Liu¹, Xibin Han¹, Yanping Chen², Jun Li^{3, 7}, Lehui Song¹, Xin Zhou⁴,
Bangqi Hu^{3, 5}, Liang Yi⁶

1. MNR Key Laboratory of Submarine Geosciences, Second Institute of Oceanography, Ministry of Natural Resources, Hangzhou 310012, China

2. Zhejiang Academy of Marine Sciences, Second Institute of Oceanography, Ministry of Natural Resources, Hangzhou 310012, China



3. MNR Key Laboratory of Marine Hydrocarbon Resources and Environmental Geology, Qingdao Institute of Marine Geology, China Geological Survey, Qingdao 266071, China


4. School of Earth and Space Sciences, University of Science and Technology of China, Hefei 230026, China

5. Laboratory for Marine Mineral Resources, Pilot National Laboratory for Marine Science and Technology, Qingdao 266071, China

6. State Key Laboratory of Marine Geology, Tongji University, Shanghai 200092, China

7. Wuhan Center, China Geological Survey, Wuhan 430205, China

 Geng Liu: <https://orcid.org/0000-0002-3253-6884>;  Bangqi Hu: <https://orcid.org/0000-0001-9397-7213>;

 Liang Yi: <https://orcid.org/0000-0003-3377-8591>

ABSTRACT: Although tropical cyclones play a critical role in global climate changes, their long-term variations in the past are not well documented. In this article, a sediment core from the South Yellow Sea was studied in order to reveal the influence of tropical cyclones on depositional processes. Integrating the results of radiocarbon dating and sediment grain-size analysis, we show that the studied sequence was deposited during the Holocene and the sedimentary dynamics were stable and at a relatively low level, with a median grain-size range of 5.3–8.7 μm . It is found that coarse particles were likely transported by highly dynamic depositional events. Based on the findings, a record of paleo-tropical cyclones was derived for the Early Holocene, and several intervals with a reduced influence of tropical cyclones were identified. In addition, it reveals a good agreement between the grain-size results and the changes in solar activity, monsoonal intensity, and the El Niño-Southern Oscillation. Overall, it can be concluded that the influence of tropical cyclones on the sedimentary evolution of the muddy zone of the South Yellow Sea was substantial during the Early Holocene on centennial timescales, and that solar maxima may control the intensity of tropical cyclones via strengthening the walker circulation over the tropical Pacific.

KEY WORDS: the Yellow Sea, Early Holocene, tropical cyclone, sedimentary process, sediment, grain size, solar activity.

0 INTRODUCTION

Several areas of muddy sediments have developed on the continental shelves of the East China Sea (i.e., the Bohai Sea and the Yellow Sea) during the Holocene (Bian et al., 2013); these muddy zones have high accumulation rates and are dominantly influenced by the Yellow and Yangtze rivers (Fig. 1). Their sediments are critical for understanding the processes by

which detrital materials are transported from land to the continental shelves (e.g., Qiao et al., 2017; Gao et al., 2016), and for this reason, they have attracted considerable research attention. Over the past decades, many studies have attempted to link sedimentary processes in these muddy zones to past changes in regional sea level, the Asian monsoon, the development of deltas, and oceanic currents (e.g., Zhang et al., 2019; Peng et al., 2018; Yang and Liu, 2007; Liu et al., 2004). For instance, by integrating shallow seismic profiling and sedimentary cores, Liu et al. (2013) proposed a close relationship between the deltaic evolution of the Yellow River and sedimentation in the South Yellow Sea. Zhou et al. (2014) reported that the relationship between sedimentary magnetic susceptibility and grain size in the South Yellow Sea can be used to identify the potential contributions of various sediment sources. Hu et al. (2012)

*Corresponding authors: bangqihu@gmail.com;
yiliang@tongji.edu.cn

© China University of Geosciences (Wuhan) and Springer-Verlag GmbH Germany, Part of Springer Nature 2022

Manuscript received June 18, 2020.

Manuscript accepted January 21, 2021.

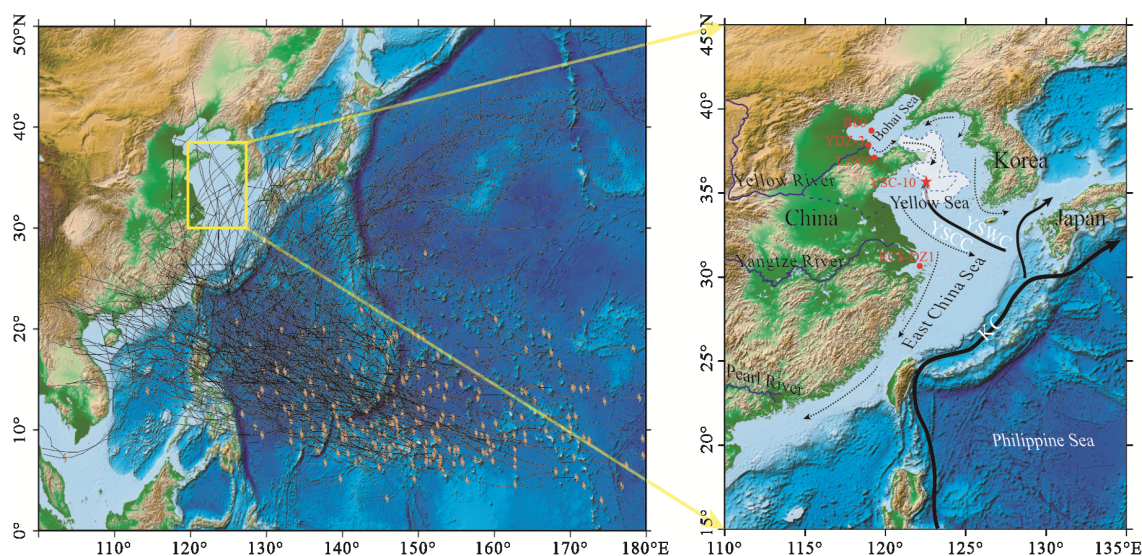


Figure 1. Typhoon tracks in the western Pacific during 1961–1997 (Ying et al., 2014) and locations of cores YSC-10 (this study), ECS-DZ1 (Chen and Li, 2018), YDZ-3 (Yi et al., 2016), Lz908 (Li et al., 2014), and B60 (Lyu et al., 2020). The solid arrows denote warm currents (YSWC, Yellow Sea warm current; KC, Kuroshio current), and the dashed arrows indicate coastal cold waters (YSCC, Yellow Sea coastal cold water). The white shaded area represents the zone of Holocene muddy sediments in the South Yellow Sea (Yang and Liu, 2007). The base map data were obtained from <http://www.ngdc.noaa.gov/mgg/global/global.html>.

found that the intervals of an intensified Asian winter monsoon identified in three sediment cores from the South Yellow Sea could be correlated to a weaken Asian summer monsoon and suggested that this was due to solar activity. He et al. (2014) reconstructed sea surface temperature (SST) variations in the center of the South Yellow Sea and proposed that a decreasing trend of SST could be linked to a weakening monsoon during the last few centuries. These findings highlight the importance of high- and mid-latitude climatic variations on sedimentary processes on the Yellow Sea.

The influence of tropical cyclones (TCs) on the sediments of these muddy zones has been relatively less explored in the previous studies (e.g., Milliman et al., 2007). The western Pacific is the most dynamical region on Earth in terms of TCs (Fig. 1), accounting for about one third of global TC generation (Henderson-Sellers et al., 1998). TCs can strengthen weathering processes and sediment fluxes (Goldsmith et al., 2008), and induce sediment erosion, transport, and re-settlement on sea floors (Yao et al., 2021; Allison et al., 2005), thereby playing an important role in global climate changes (Emanuel, 2005; Webster et al., 2005). In the context of global warming, TCs are becoming significantly more intense according to modern observations and numerical modeling (Pausata and Camargo, 2019; Zhou X et al., 2019; Tu et al., 2009; Wada and Usui, 2007); however, several researchers have argued that no significant correlation exists between SST and TC intensity (Chan and Liu, 2004). Due to short-term observations, geological archives can provide critical insights into TCs and enable the testing of various hypotheses of the relationship between TC activity and global climate changes (e.g., Shan et al., 2019; Tian et al., 2019; Zhang et al., 2018; Huang et al., 2015; Wang L C et al., 2014; Woodruff et al., 2009). For instance, McCloskey and Liu (2013, 2012) reported two cases of Holocene paleo-hurricane activity by studying the sedimentary characteristics in coastal areas of Central America, and found that hurricane behaviors varied across the

basin. For the Late Holocene, Chen et al. (2019, 2012) reconstructed changes in paleo-typhoons which were closely correlated to El Niño–Southern Oscillation (ENSO) activity. Zhou L et al. (2019, 2017) validated the potential of coastal lagoon deposits for reconstructing paleo-typhoon events during the Middle to Late Holocene, and reported that both ENSO and Western Pacific Warm Pool have modulated paleo-typhoon changes.

However, most previous studies have focused on the Late Holocene and there are few studies of the more distant past (e.g., Huang et al., 2015); this hinders our understanding of how tropical climate conditions, such as TC activity, were influenced by mid-latitude environmental processes in the past. Therefore, in the present study, we attempt to reconstruct paleo-TC variability in the Early Holocene using grain-size analysis of a sediment core from the South Yellow Sea (Fig. 1), with the aim of detecting its potential linkage with various key climatic processes.

1 MATERIALS AND METHODS

1.1 Sediment Core YSC-10

The studied sediment core, YSC-10 (122°25'E, 35°58'N), was collected from the South Yellow Sea (Fig. 1). The sediments in the area are transported mainly by the Yellow River in winter, under the influence of the Yellow Sea warm current (YSWC) and Yellow Sea cold current (YSCC) (Liu et al., 2013; Shen et al., 1993); the YSWC is one of the major branches of the Kuroshio current (KC). In addition, suspended sediments from the Yangtze River may be carried back into the South Yellow Sea (Sun et al., 2000), driven by the YSWC and the south-east summer monsoon (Zou et al., 2001; Tang et al., 2000).

Core YSC-10 was obtained in 2015 by the Qingdao Institute of Marine Geology, using a gravity driller with a diameter of 130 mm. The water depth in the area is 56.8 m, and the length of the core is 454 cm. The core sediments are highly homogeneous, grayish and blue-gray, consisting of clay and silty particles; there are only minor lithological changes with depth. For

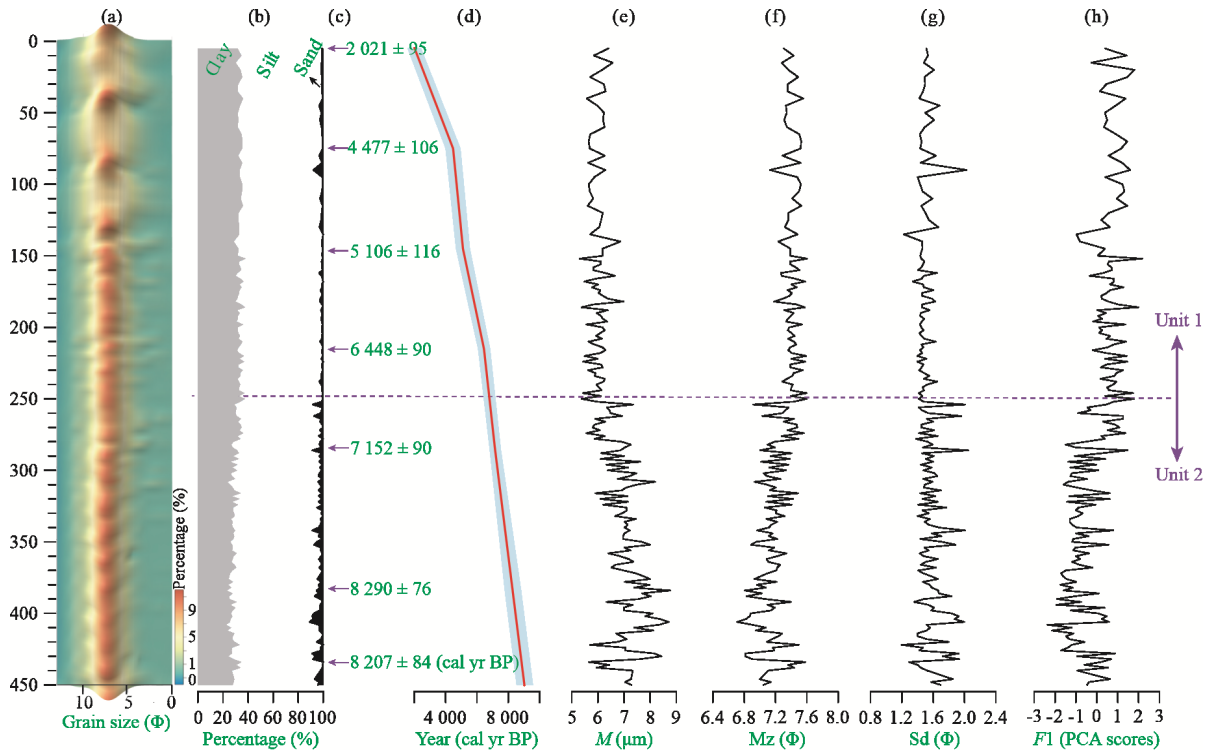


Figure 2. Grain-size distributions, chronology, grain-size parameters, and VPCA results for core YSC-10. (a) Grain-size frequency distributions; (b) percentages of clay (<4 μm), silt (4–63 μm), and sand (>63 μm); (c) AMS ¹⁴C dating results with 1σ uncertainties; (d) age model with 95% confidence intervals plotted as light blue shading; (e)–(h) parameter changes in sediment grain size of core YSC-10. *M*. Median size; *Mz*. mean size; *Sd*. standard deviation; *F1*. the leading component (39.47%; Fig. 3b).

grain-size analysis, the core was sampled in the laboratory at 5 and 2 cm intervals for the depths of 0–150 and 150–454 cm, respectively.

1.2 Laboratory Analyses

Seven samples of mixed planktonic foraminifera from core YSC-10 were extracted for radiocarbon dating (Fig. 2). The radiocarbon measurements were conducted by Beta Analytic Inc. USA using accelerator mass spectrometry (AMS). To remove the effects and the influence of stable carbon isotope (Reimer et al., 2016), the AMS ¹⁴C dates were calibrated using Calib7.1 (Stuiver et al., 2019), with an additional regional reservoir correction ($\Delta R = -138 \pm 68$ yr) (Liu et al., 2016; Ye et al., 1989).

A total of 178 grain size samples were measured for paleoenvironmental study. The grain size samples were pretreated with 10–20 mL of 30% H₂O₂ to remove organic matter, washed with 10% HCl to remove carbonates, rinsed with deionized water, and then placed in an ultrasonic bath for several minutes to facilitate dispersion. The grain size spectra of the remaining terrigenous material were measured using a Malvern Mastersizer 2000 laser-particle size analyzer at the School of Geographic and Oceanographic Sciences, Nanjing University, China. A total of 100 grain size ranging of 0.3–600 μm were exported for further analysis.

Sediment grain-size analysis is a power tool in paleoenvironmental studies (e.g., Manoj et al., 2020; Liang et al., 2017; Zhang et al., 2017). For analyses of sedimentary dynamics, two parameters were selected: the *C* value, which is one percentile of grain size distribution and indicates the most hydro-

dynamic sedimentary component; and the *M* value, which is the median diameter and reflects the mean hydrodynamic energy. The *C*–*M* diagram can provide valuable insights into sediment transport and hydrodynamic intensity (Passega, 1964, 1957). In order to identify the factors associated with sedimentary grain-size changes and to extract potential paleoenvironmental signals, we analyzed the grain-size spectra using a varimax-rotated, principal component analysis (VPCA), which can partition various sediment inputs or dynamics components (e.g., Yi et al., 2016). We also used core Lz908 from the Bohai Sea (Li et al., 2014), core YDZ-3 from the modern delta of the Yellow River (Yi et al., 2016), and core ECS-DZ1 from the East China Sea (Chen et al., 2020), as references to cross-check the results from core YSC-10.

2 RESULTS AND DISCUSSION

2.1 Age Model

Reference to Table 1 shows that most of AMS ¹⁴C dates increase with depth (Fig. 2c), suggesting that the sedimentary processes were relatively stable during the interval of sediment accumulation. The topmost age (2 021 cal yr BP) at 5 cm depth is consistent with previous reports (Mei et al., 2016; Wang F F et al., 2014), which documented substantial hiatuses along the margins of the muddy zone in the South Yellow Sea. Although the basal date (8 207 ± 84 cal yr BP) is slightly younger than the preceding date (8 290 ± 76 cal yr BP), there is an overall good consistency between date and depth ($r = 0.97$, $p < 0.01$) for core YSC-10, which demonstrates the reliability of the geochronology obtained by linear interpolating between the radio-

Table 1 Radiocarbon dating on the materials from core YSC-10

Sample ID	Lab No.	Depth (cm)	Dating materials	Conventional age \pm error (yr BP)	Calibrated age \pm error (cal yr BP)	95% confidence interval (cal yr BP)
YSC10-5	444549	5		2 250 \pm 30	2 021 \pm 95	1 841–2 246
YSC10-75	444550	75		4 200 \pm 30	4 477 \pm 106	4 244–4 713
YSC10-145	444551	145	Mixed planktonic foraminifera	4 680 \pm 30	5 106 \pm 116	4 879–5 290
YSC10-215	444552	215		5 890 \pm 30	6 448 \pm 90	6 289–6 621
YSC10-285	444553	285		6 490 \pm 30	7 152 \pm 90	6 958–7 307
YSC10-385	444554	385		7 690 \pm 40	8 290 \pm 76	8 134–8 439
YSC10-435	444555	435		7 600 \pm 30	8 207 \pm 84	8 027–8 352

Table 2 One-way ANOVA results for grain-size parameters of core YSC-10

	Variance	Sum of squares	Mean square	<i>F</i> value	Sig. level
<i>M</i>	Between groups	33.5	33.5	83.0	<0.01
	Within groups	71.0	0.4		
	Total	104.5			
<i>Mz</i>	Between groups	2.0	2.0	69.4	<0.01
	Within groups	5.1	0.03		
	Total	7.1			
<i>Sd</i>	Between groups	0.3	0.3	12.6	<0.01
	Within groups	3.7	0.02		
	Total	4.0			
<i>C</i>	Between groups	130 281	130 281	13.5	<0.01
	Within groups	1 701 308	9 666		
	Total	1 831 589			
>125 μm	Between groups	27.5	27.5	15.1	<0.01
	Within groups	319.9	1.8		
	Total	347.5			
<i>F1</i>	Between groups	47.9	47.9	65.4	<0.01
	Within groups	129.1	0.7		
	Total	177.0			
<i>F3</i>	Between groups	9.0	9.0	9.4	<0.01
	Within groups	168.0	1.0		
	Total	177.0			

carbon dates (Fig. 2d). The resulting sediment accumulation rates are close to regional estimates (Zhang et al., 2019), indicating that the basal age of core YSC-10 is \sim 9 000 cal yr BP (Liu et al., 2020).

2.2 Sediment Grain Size Changes

The mean sediment grain size (*Mz*) for the entire core is $7.3 \pm 0.2 \Phi$ (Fig. 2). This value indicates the occurrence of low-energy sedimentary processes during the Holocene, and in addition the low standard deviation confirms that in terms of grain size the sediments are relatively homogenous. However, most of the grain-size parameters, such as the contents of clay ($<4 \mu\text{m}$), silt ($4-63 \mu\text{m}$), and sand ($>63 \mu\text{m}$), show a pronounced shift at the depth of \sim 250 cm (Fig. 2). Specifically, in the upper part of the core (Unit 1), the *Mz*, median size (*M* value), and standard deviation (*Sd*) are $7.4 \pm 0.1 \Phi$, $6.0 \pm 0.3 \mu\text{m}$, and $1.5 \pm 0.1 \Phi$, respectively, with a sandy content of $1.3\% \pm 1.1\%$; and in the lower part of the core (Unit 2), the correspond-

ing values are $7.1 \pm 0.2 \Phi$, $7.0 \pm 0.7 \mu\text{m}$, and $1.6 \pm 0.2 \Phi$, respectively, and the sandy content is $3.0\% \pm 2.5\%$. To confirm that there is a statistically significant difference between the two units, we conduct one-way analysis of variance (ANOVA) for several grain-size parameters. As shown in Table 2, all of the differences between the two units are statistically significant ($p < 0.01$), inferring that the boundary between the two units represents a significant change in sedimentary processes.

A multi-mode grain-size distribution pattern is evident in the data from core YSC-10, which was also observed in other cores from the continental shelves of the East China Sea, but with different modal values (Fig. 3a). Moreover, this multi-mode pattern of grain-size distribution does not change significantly with depth in the core (Fig. 2a), confirming the stability of sedimentary processes during the Holocene. The VPCA results of the grain-size data identify three characteristic components (Fig. 3b), which accounts for 91.10% of the total variance (Table 3). The first two leading components likely integrate variations of low-dynamic sedimentary processes (Fig. 3b), while the third component, which is correlated with the $>150 \mu\text{m}$ grain-size fraction, reflects a high-energy sedimentary process which is more energetic than those previously identified in coastal and fluvial sediments of the Bohai Sea and the East China Sea (Fig. 3a). Notably, the *C-M* diagram displays a different pattern compared to that for the Bohai Sea and the East China Sea, with *C* values of 30–500 μm and *M* values of 5.3–8.7 μm (Fig. 3d). These results show that the most dynamic sedimentary process recorded in core YSC-10 does not track the variations in the dominant sedimentary components.

2.3 Index of Tropical Cyclone Activity

2.3.1 Possible environmental processes responsible for the grain-size characteristics

Paleo-TC records have usually been identified based on a disturbed depositional sequence or a high-dynamic sedimentary event (e.g., Zhou et al., 2017; Huang et al., 2015; Wang L C et al., 2014; Woodruff et al., 2009). For instance, Woodruff et al. (2009) reconstructed Middle to Late Holocene typhoon variability by identifying the sedimentary signature of coastal flooding in Japan. Similarly, Wang L C et al. (2014) estimated paleo-TC influences using coarse-grained sediments and planktonic diatoms in Taiwan Island. Most recently, Zhou X et al. (2019) studied paleo-TC variability over the past 2 000 years using variations of the coarse fraction ($>63 \mu\text{m}$) of sediment cores collected from the muddy zone in the East China Sea, and found a close relationship between paleo-TC variability

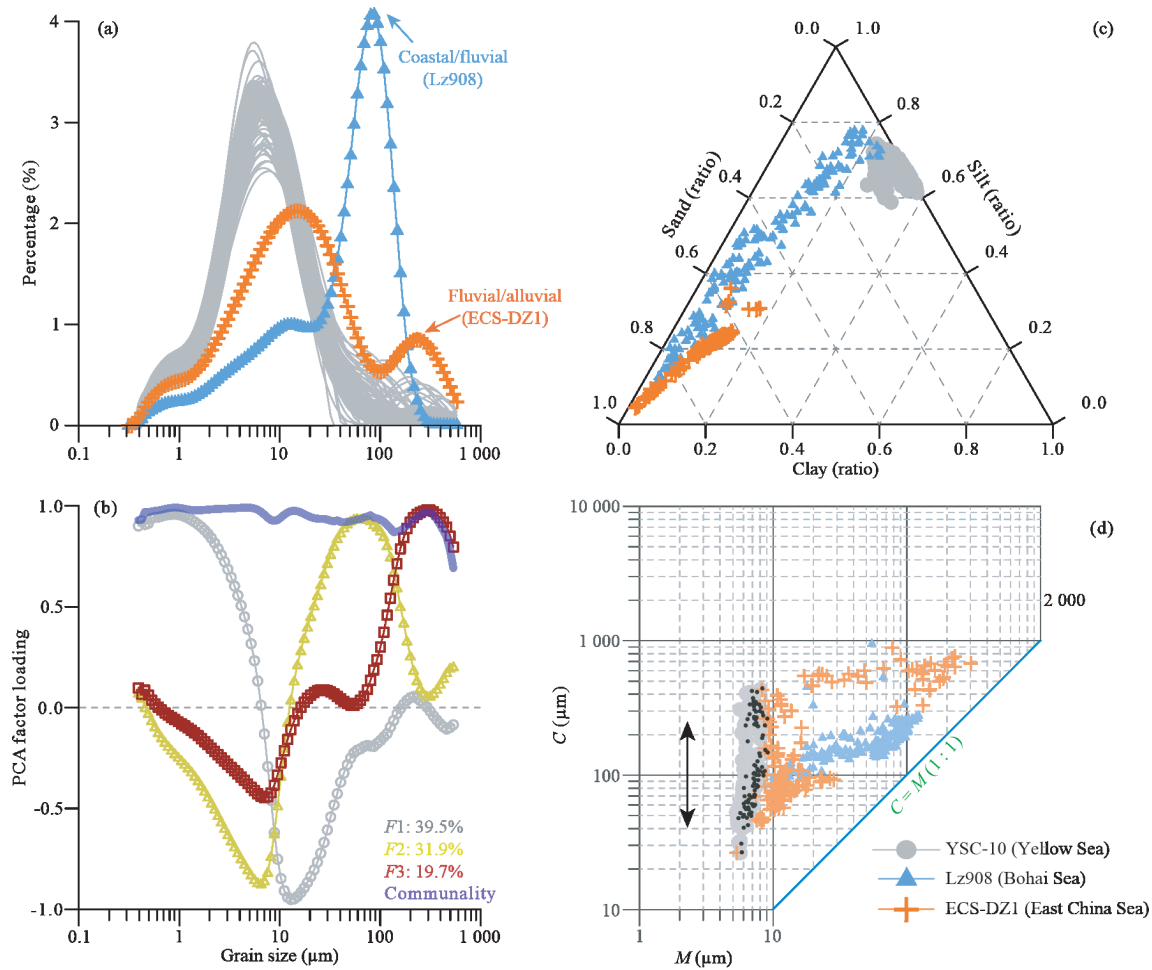


Figure 3. Comparison of sediment grain-size characteristics of various depositional environments. (a) Grain size distribution of core YSC-10 (this study), core Lz908 (Bohai Sea; Li et al., 2014), and core ECS-DZ1 (East China Sea; Chen et al., 2020); (b) VPCA factor loadings for the grain-size data from core YSC-10; (c) ternary diagrams for the grain-size data from the three sediment cores; (d) corresponding *C-M* diagrams.

Table 3 Results of principal component analysis of sediment grain-size of core YSC-10

Component	Initial eigenvalues/extraction		
	Total	% of Variance	Cumulative %
<i>F1</i>	38.28	39.47	39.47
<i>F2</i>	30.98	31.94	71.41
<i>F3</i>	19.10	19.69	91.10

and global warming. On this basis, changes in the coarse fraction could potentially reflect TC activity in the East China Sea.

Due to regional oceanic currents and the strong influence of the Yellow River (e.g., Yang and Liu, 2007; Liu et al., 2004), fine-grained sediments are deposited in the study area and areas of muddy sediments developed (Bian et al., 2013). As mentioned above, the median grain size of core YSC-10 is $6.6 \pm 0.8 \mu\text{m}$, suggesting a very low-energy hydrodynamic environment in the study area during the Holocene. Under the influence of tropical cyclones (Fig. 1), coarse particles in such an environment have two possible sources, river inputs and transport by TCs.

The Yellow River is one of the main sediment sources of the South Yellow Sea (Shen et al., 1993), and the median size of the sediments at the modern river mouth ranges from 30 to

$50 \mu\text{m}$ (Ren et al., 2012); in addition, sedimentary inputs of the Yellow River into the Bohai Sea are closely correlated with monsoonal changes (Yi et al., 2016). It can be seen that there is some consistency between the Asian monsoon variations (Fig. 4a) and the sedimentary record of core YSC-10 (Fig. 4b), inferring that the Asian monsoon played an important role in the sedimentary evolution of the studied area. Moreover, the study area is a part of the subaqueous delta of the Yellow River in the South Yellow Sea (Liu J et al., 2013; Yang and Liu, 2007; Liu J P et al., 2004), and the deltaic evolution of the Yellow River is another important sedimentary influence. After the initiation of the Yellow River Delta at $\sim 6300 \text{ yr BP}$ (Yi et al., 2016), the average sediment accumulation rate in core YSC-10 decreased from ~ 0.93 to $\sim 0.47 \text{ m/kyr}$ after $\sim 6500 \text{ yr BP}$. Since detrital materials might be trapped due to the formation of the Yellow River Delta, the decreased sedimentation rate may be associated with its formation (Liu et al., 2020), which is also the case for the delta of the Yangtze River (e.g., Wang L C et al., 2014).

Sea-level change is another critical factor that may have influenced the sedimentary evolution of the study area. In the Early Holocene, the rapid rise of global sea level ceased (Fig. 4f), and the level was 10–20 m below that of today (Waelbroeck et al., 2002), or close to it (Siddall et al., 2003). A re-

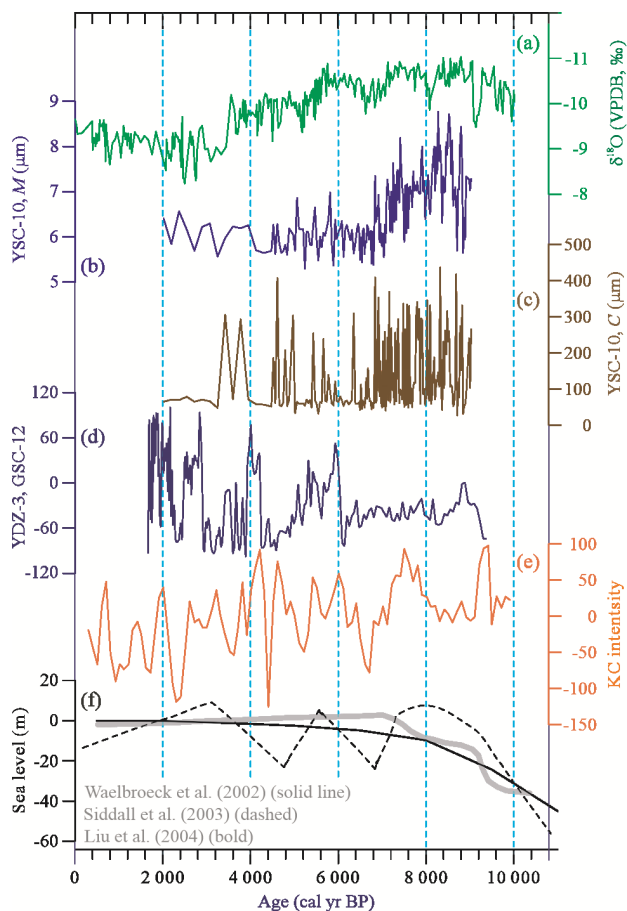


Figure 4. Comparison of various environmental proxy records from East Asia. (a) Stalagmite $\delta^{18}\text{O}$ series from Sanbao Cave (Cheng et al., 2016), indicating Asian monsoon intensity; (b)–(c) sediment grain-size changes in core YSC-10 (this study); (d) sediment grain-size changes of core YDZ-3 (Yi et al., 2016), indicating the deltaic evolution of the Yellow River; (e) stack record of the Kuroshio current (KC), based on four time series (Jian et al., 2000) integrated using VPCA (Yi et al., 2016); (f) global and regional sea level changes during the Holocene.

gional sea-level reconstruction for the East China Sea shows a similar pattern (Liu et al., 2004). For core ECS-DZ1 (water depth ~12 m), close to the mouth of the Yangtze River (Fig. 1), the median size of the coarse particles is ~250 μm (Fig. 3a), while for core YSC-10 (water depth ~57 m), far from the coastline of Jiangsu and Shandong provinces, the median size of the coarse particles is ~314 μm (Fig. 3). Considering the small range of variations of the M value and the VPCA component $F1$ (Fig. 2), together with the core location, sea-level changes may have had a relatively weak influence on the sedimentary dynamics of the study area. Additionally, there is no agreement between the changes in C values of core YSC-10 and the KC (Fig. 4e), of which the YSWC is one of the main branches in the South Yellow Sea. It has been suggested that although the KC dominates the chemical characteristics of the muddy zone (Zhang et al., 2019; He et al., 2014), this is not the case for the sedimentary dynamics.

Overall, the variations of these three factors—the Asian monsoon, deltaic evolution, and regional sea-level change—have minimal consistency with the stratigraphic variation of

coarse particles in the study area (Fig. 4c). Notably, the C value is the most dynamic sedimentary component of core YSC-10, implying that other factors may dominate the sedimentary process responsible for its transport.

2.3.2 TC index

The C - M diagram for core YSC-10 is quite different to that for other locations in the region (Fig. 5). For suspended and sea-surface sediments around the modern mouth of the Yellow River (Figs. 5b, 5c) and in the muddy zone of the Bohai Sea (Fig. 5e), there is a good positive correlation between C and M values. This is also evident for cores Lz908 and ECS-DZ1 (Chen and Li, 2018; Li et al., 2014), as well as for sediments from the abandoned mouth of the Yellow River in the western part of the South Yellow Sea (Fig. 5d). The covariation of M and C indicates that the most dynamic component is usually integrated with the mean state of sedimentary processes for various environments, and this relationship was observed in the first application of the C - M diagram to different sedimentary facies and depositional periods (Passega, 1964, 1957). By contrast, in core YSC-10, C varies independently of M (Fig. 5a), which suggests that the most dynamic component should reflect the effects of some undetected factor. This unique pattern does not reflect a response to the Asian monsoon, the Yellow River, or to regional sea-level changes, but it suggests the possible role of other highly dynamic events, such as TC transport.

TCs are a major factor affecting the sea-floor geomorphology and sediment redeposition in coastal zones and continental shelves (Zhou X et al., 2019; Huang, 2017; Sun et al., 2017; D'Asaro et al., 2014). For instance, because of their large wavelength and high energy, the influence of tropical cyclones can extend to water depths of >100 m (Wang et al., 2018; Hale et al., 2012), resulting in coarse particles being transported far from the coastlines. Because of the long distance to the coastlines in the muddy zone of the South Yellow Sea (Fig. 1), coarse particles cannot readily be supplied by rivers and currents, and TCs are the most likely transport medium. Moreover, as a sediment transport agent, TCs differ from rivers and currents which usually determine the mean state of sedimentary dynamics; by contrast, TCs represent episodic and random impacts, which are relatively independent of the influence of rivers and currents. This characteristic is likely to be responsible for the observation that C varies independently of M in core YSC-10. Therefore, considering the relatively low deposition rate and large sampling interval in the upper part of core YSC-10, we now focus on the lower part of the core (below ~226 cm, prior to ~6 558 cal yr BP), and use the coarse fraction to reflect variations in the intensity of TCs and to explore their variability.

Typically, three of the studied grain-size parameters represent changes in coarse particles, i.e., the C value, the sandy content (>125 μm), and VPCA $F3$. Specifically, the C value represents the intensity of the most dynamic component (Fig. 6a); the sandy content represents the contribution of coarse particles to the grain-size distribution (Fig. 6b); and VPCA $F3$ represents the pattern of variations of coarse particles (Fig. 6c). Because of the high degree of consistency between the three parameters, we used their arithmetic mean and standardized value to reduce

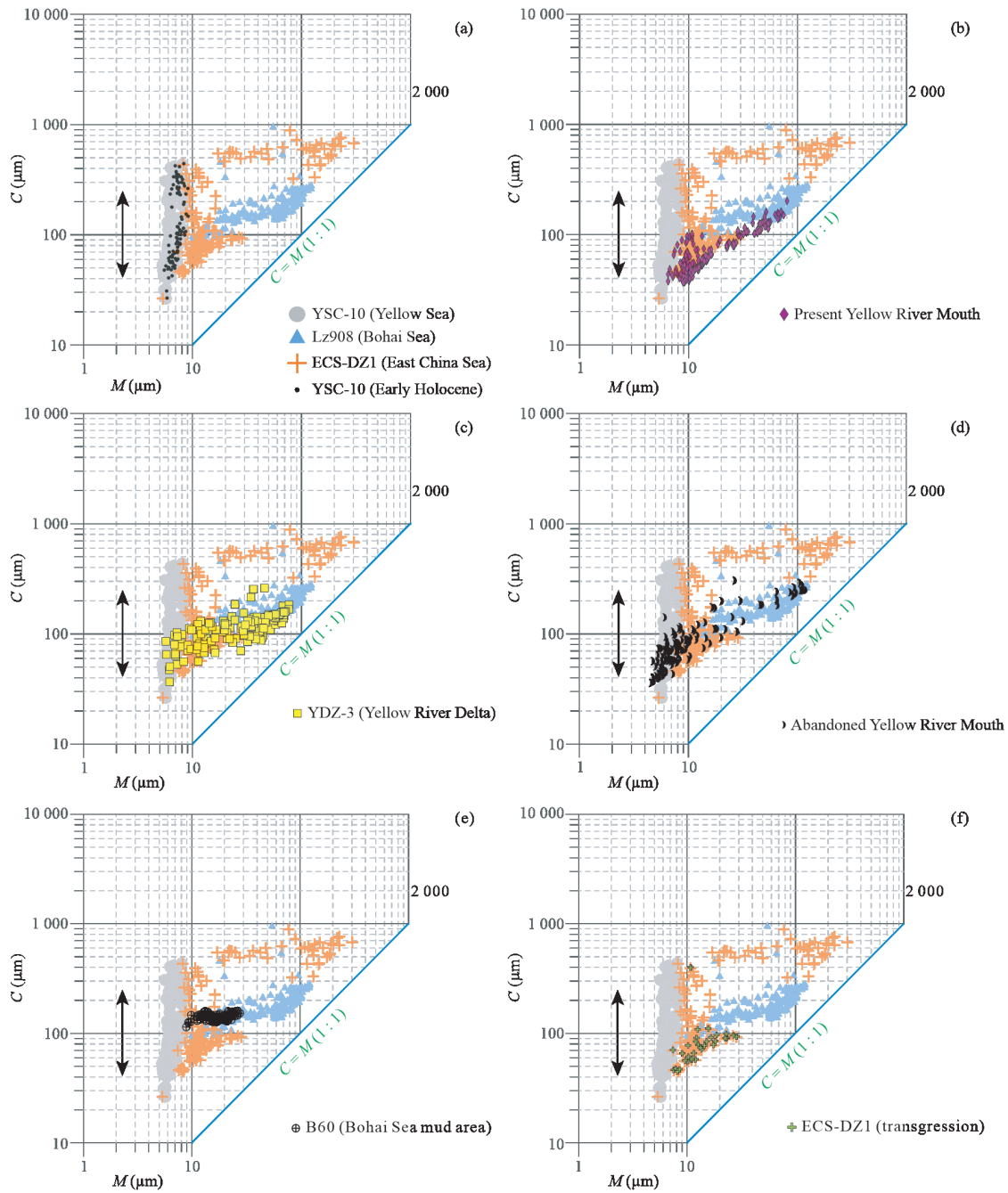


Figure 5. *C-M* diagrams for marine sediment from various environments. (a) *C-M* changes of core YSC-10 during the Early Holocene (this study), highlighted by black dots; (b) surface sediments from the modern mouth of the Yellow River Mouth (Ren et al., 2012); (c) sediments of core YDZ-3 from the present Yellow River Delta (Yi et al., 2016); (d) surface sediments of the abandoned mouth of the Yellow River in the western part of the South Yellow Sea (Zhang et al., 2014); (e) sediments of core B60 from the central muddy zone of the Bohai Sea (Lyu et al., 2020); (f) *C-M* changes in core ECS-DZ1 during the Early Holocene (Chen et al., 2020), highlighted as green crosses.

the potential bias involved in using a single index

$$x_i = \frac{x_i - \min}{\max - \min}; \text{TC} = \frac{\sum x_i}{n}$$

Here x_i represents the three grain-size indices, $n = 3$, and TC is the derived index of tropical paleo-cyclones. The resulting TC index represents major changes in the hydrodynamic in the South Yellow Sea (Fig. 6d), and reference to Fig. 7 reveals substantial centennial-scale variability of this signal during the Early Holocene.

2.4 Variation in the TC Index and Its Potential Driving Mechanism

The TC index can be used to examine temporal variations in the influence on sedimentation in the South Yellow Sea during the Early Holocene, and its relationship with other factors (Figs. 6–8). Four periods with relatively low intensity of paleo-TC are evident: 6 500–6 800, 7 200–7 500, 7 900–8 400 cal yr BP, and prior to 8 800 cal yr BP, with 100–300-year periodicities (Fig. 7). These intervals with low paleo-TC intensity can

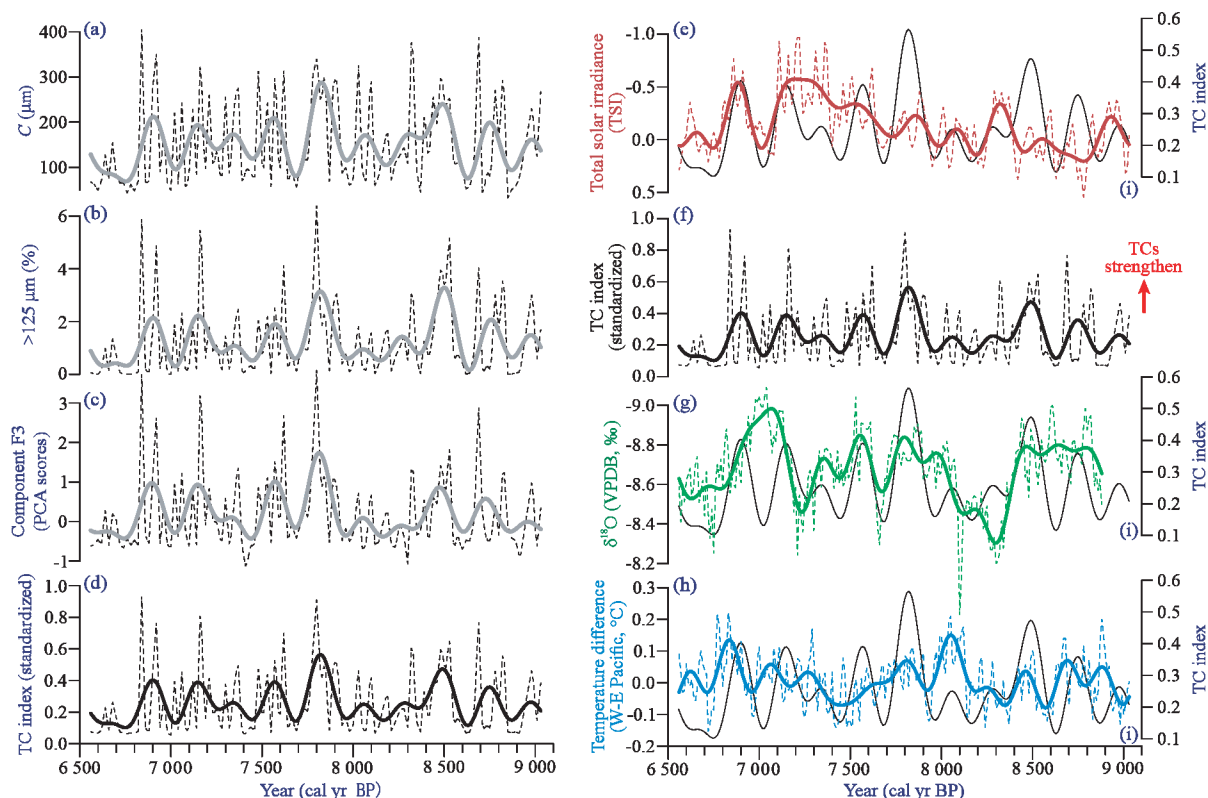


Figure 6. Derived tropical cyclone (TC) activity in the Yellow Sea and comparisons with various environmental proxies. (a)–(c) *C*-value, >125 µm content, and VPCA *F3* of core YSC-10 with FFT low-frequency (<0.005) components (bold lines); (d), (f) Stacked grain-size index reflecting strong sedimentary dynamics associated with tropical cyclone (this study), and (i) FFT low-frequency (<0.005) component of (d), (f); (e) total solar irradiance (TSI) during the Holocene (Steinhilber et al., 2009); (g) stalagmite $\delta^{18}\text{O}$ record from Dongge Cave (Wang et al., 2005), indicating Asian monsoon intensity; (h) SST difference between the western and eastern Pacific (Emile-Geay et al., 2007), indicating ENSO-like conditions. All dashed lines represent the original data, and the bold lines represent their FFT low-frequency (<0.005) components.

be linked to Asian monsoon weakening events (Cheng et al., 2016; Wang et al., 2005) in the Early Holocene; however, there is little consistency between the original time series (Fig. 4a), except on the centennial timescales (Figs. 6i and 8). Modern observations show that the average rainfall associated with tropical cyclones exceeds 700 mm/year (Wang et al., 2008), which contributes to 60%–80% of the variance of annual/summer rainfall in eastern China (Yi et al., 2018). Considering these observations, Yi et al. (2018) suggested that on orbital timescales, TCs may have significantly contributed to Asian monsoon variability during the Late Quaternary. Our data from the South Yellow Sea suggest that changes in the TC index and Asian monsoon may not be directly correlated on the centennial timescales, but the agreement between the low-frequency filtered versions of these signals (>200-yr periodicity) indicates a close relationship between them, which is worth investigating in the future.

According to modern observations, TCs are controlled by tropical SST in the western Pacific, where local SSTs are usually higher than 26–27 °C, and below this temperature threshold their generation decreases abruptly to an extremely low level (Wada and Usui, 2007). In the tropical Pacific, the most prominent factor affecting SST changes is ENSO (Cai et al., 2019), which is defined by the SST difference between the western and eastern Pacific and varies between warm states (El Niño) and cold states (La Niña). The ENSO influence on tropical cyclones generation/intensity is complicated. For instance, using

modern typhoon data and historical documents from South China, Elsner and Liu (2003) proposed that TCs tend to recur northward, away from China, during an El Niño event (e.g., Bian et al., 2013; Chan, 2000, 1985). By contrast, Camargo and Sobel (2005) argued that TCs are more intense and longer-lived during El Niño years than La Niña years, according to an analysis of the statistical relation among observation data. Kang et al. (2019) stated that the differences in the spatial distribution of the locations of TC genesis were not solely determined by different ENSO states. However, conclusions derived from reconstructions of the paleo-TC variation from geological records tend to be similar. For example, Chen et al. (2012) observed that an intensified paleo-TC occurred more frequently during La Niña-like states; and Zhou L et al. (2019) found a positive correlation between paleo-TC intensity and La Niña-like intervals in the South China Sea. In the present study, there is a good agreement between the TC index and the SST difference between the western and eastern Pacific (Figs. 6h and 8), which supports the hypothesis that TCs are more intense and longer-lived during La Niña years. Over the past decades, the increased temperature difference between the western and eastern Pacific during an La Niña state would intensify the Walker circulation and monsoonal rainfall over East Asia (Emile-Geay et al., 2007), and TC influences over East Asia would similarly be strengthened (Chen et al., 2012; Ma et al., 2006). On the centennial timescale, this relationship may be similar, demon-

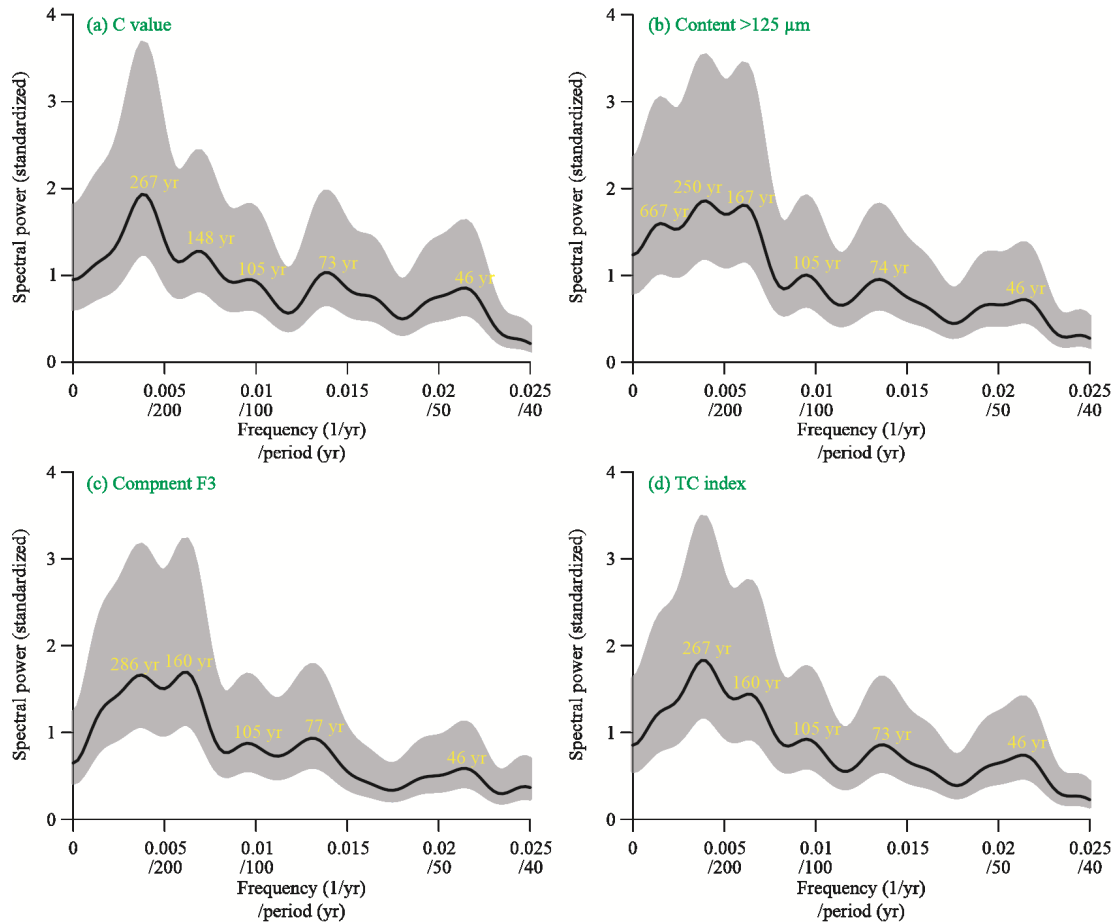


Figure 7. Results of Blackman-Tukey spectral analysis of TC-related proxies. Significant periodicities are labelled, and the shaded area indicates the 80% confident interval. The spectra were obtained using ARAND software (Howell et al., 2006).

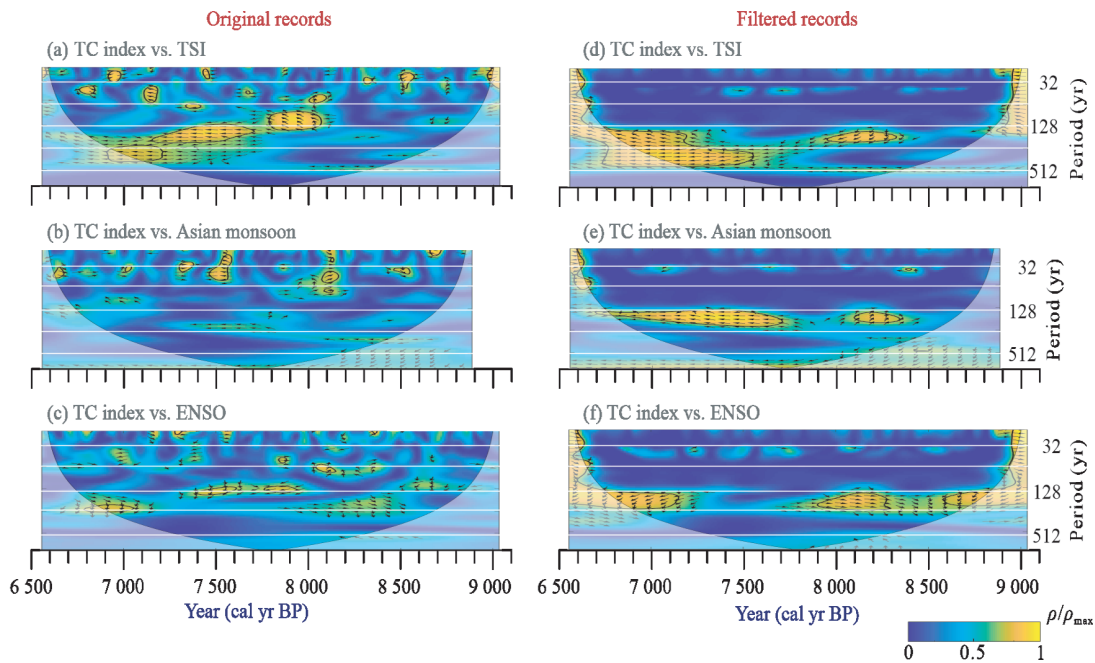


Figure 8. Squared wavelet coherence (WTC; Grinsted et al., 2004) between a stacked high-sedimentary-dynamic grain-size index indicating tropical cyclone (TC) activity and total solar irradiance (a), (d), and the stalagmite $\delta^{18}\text{O}$ record from Dongge Cave (b), (e), and the SST difference between the western and eastern Pacific (c), (f). The 5% significance level against red noise is shown as a thick contour. All significant sections show in-phase behavior (with in-phase pointing right, anti-phase pointing left). WTC in the right panel is calculated using FFT low-frequency components, while in the left panel using the original data.

strating a consistent relation between ENSO, the Asian monsoon, and paleo-TC intensity.

Previous studies have shown that solar activity is one of the most important factors in regional climate changes during the Holocene (e.g., Tan et al., 2011; Wang et al., 2005; Bond et al., 2001); however, the influence of solar activity on climate changes in the tropical Pacific is debated. On decadal timescales, for example, Meehl et al. (2009) revealed that solar maxima could enhance the off-equatorial tropical rainfall and reduce tropical clouds. Misios et al. (2019) reported a reduced hydrological cycle that weakens the Walker circulation over the tropical Pacific during solar maxima, which is likely amplified by the Bjerknes feedback. Wang et al. (2005) suggested that on decadal to centennial timescales, higher solar irradiance corresponded to stronger Asian monsoon intensity, based on the stalagmite $\delta^{18}\text{O}$ record of Dongge Cave in South China. In this study, the observed good agreement between the paleo-TC record and reconstructed total solar irradiance (TSI), which represents variations in solar activity (Figs. 6e and 8), confirms that solar activity may be one of the most important factors controlling past changes in TC intensity. Integrating all of these comparisons, it is proposed that solar maxima may strengthen the Walker circulation over the tropical Pacific and thus intensify TC and Asian monsoon during the Early Holocene.

3 CONCLUSIONS

The radiocarbon dating and sediment grain-size analyses of a sedimentary sequence from the South Yellow Sea are used to reconstruct the influence of tropical cyclones on sedimentation during the Early Holocene. The main findings are as follows.

(1) The studied core was deposited during the Holocene and its sedimentary dynamics were relatively weak and uniform, with a median grain size range of $\sim 5.3\text{--}8.7\ \mu\text{m}$.

(2) The coarse fraction of the sediments was likely transported by highly energetic sedimentary events, based on a comparison of the grain-size characteristics with those of sediments of the Bohai Sea and East China Sea.

(3) A paleo-tropical cyclone record was derived from the content of coarse particles ($>125\ \mu\text{m}$) in the sediments; the variations in this record are correlative with changes in solar activity, monsoonal intensity, and the El Niño-Southern Oscillation.

(4) The influence of tropical cyclones on the sedimentary evolution of the muddy zone of the South Yellow Sea was significant on the centennial timescale in the Early Holocene, and solar maxima may have controlled the intensity of tropical cyclones by strengthening the Walker circulation over the tropical Pacific.

ACKNOWLEDGMENTS

The authors thank Prof. Jianhua Gao from Nanjin University of China for providing helps in sediment grain-size measurements, and three anonymous reviewers for their suggestion and comments in improving this manuscript. This work was supported by the National Key R&D Program of China (No. 2018YFE0202401), the National Natural Science Foundation of China (Nos. 41602349 and 41976192), and the Marine S&T Fund of Shandong Province for Pilot National Laboratory for Marine Science and Technology (Qingdao) (No. 2022QNLMO50203). All data supporting the findings of this study are available at [\[vliz.be/directlink.php?fid=VLIZ_00000824_6270c53c44bed859352062\]\(https://doi.org/10.1007/s12583-021-1417-z\). The final publication is available at Springer via <https://doi.org/10.1007/s12583-021-1417-z>.](https://mda.</p>
</div>
<div data-bbox=)

REFERENCES CITED

- Allison, M. A., Sheremet, A., Goñi, M. A., et al., 2005. Storm Layer Deposition on the Mississippi-Atchafalaya Subaqueous Delta Generated by Hurricane Lili in 2002. *Continental Shelf Research*, 25(18): 2213–2232. <https://doi.org/10.1016/j.csr.2005.08.023>
- Bian, C. W., Jiang, W. S., Greatbatch, R. J., 2013. An Exploratory Model Study of Sediment Transport Sources and Deposits in the Bohai Sea, Yellow Sea, and East China Sea. *Journal of Geophysical Research: Oceans*, 118(11): 5908–5923. <https://doi.org/10.1002/2013jc009116>
- Bond, G., Kromer, B., Beer, J., et al., 2001. Persistent Solar Influence on North Atlantic Climate during the Holocene. *Science*, 294(5549): 2130–2136. <https://doi.org/10.1126/science.1065680>
- Cai, W. J., Wu, L. X., Lengaigne, M., et al., 2019. Pantropical Climate Interactions. *Science*, 363(6430): eaav4236. <https://doi.org/10.1126/science.aav4236>
- Camargo, S. J., Sobel, A. H., 2005. Western North Pacific Tropical Cyclone Intensity and ENSO. *Journal of Climate*, 18(15): 2996–3006. <https://doi.org/10.1175/jcli3457.1>
- Chan, J. C. L., 1985. Tropical Cyclone Activity in the Northwest Pacific in Relation to the El Niño/Southern Oscillation Phenomenon. *Monthly Weather Review*, 113(4): 599–606. [https://doi.org/10.1175/1520-0493\(1985\)113<0599:tcaint>2.0.co;2](https://doi.org/10.1175/1520-0493(1985)113<0599:tcaint>2.0.co;2)
- Chan, J. C. L., 2000. Tropical Cyclone Activity over the Western North Pacific Associated with El Niño and La Niña Events. *Journal of Climate*, 13(16): 2960–2972. [https://doi.org/10.1175/1520-0442\(2000\)013<2960:tcaotw>2.0.co;2](https://doi.org/10.1175/1520-0442(2000)013<2960:tcaotw>2.0.co;2)
- Chan, J. C. L., Liu, K. S., 2004. Global Warming and Western North Pacific Typhoon Activity from an Observational Perspective. *Journal of Climate*, 17(23): 4590–4602. <https://doi.org/10.1175/3240.1>
- Chen, H. F., Wen, S. Y., Song, S. R., et al., 2012. Strengthening of Paleotyphoon and Autumn Rainfall in Taiwan Corresponding to the Southern Oscillation at Late Holocene. *Journal of Quaternary Science*, 27(9): 964–972. <https://doi.org/10.1002/jqs.2590>
- Chen, H. F., Liu, Y. C., Chiang, C. W., et al., 2019. China's Historical Record when Searching for Tropical Cyclones Corresponding to Intertropical Convergence Zone (ITCZ) Shifts over the Past 2 kyr. *Climate of the Past*, 15(1): 279–289. <https://doi.org/10.5194/cp-15-279-2019>
- Chen, Y. P., Li, Y., 2018. Sediment Grain-Size Characteristics and Sediment Significance of DZ-1 Borehole near Zhoushan Islands, East China Sea. *Journal of Marine Sciences*, 36(4): 53–59. <https://doi.org/10.3969/j.issn.1001-909x.2018.04.007> (in Chinese with English Abstract)
- Chen, Y. P., Li, Y., Lyu, W. Z., et al., 2020. A 5 000-Year Sedimentary Record of East Asian Winter Monsoon from the Northern Muddy Area of the East China Sea. *Atmosphere*, 11(12): 1376. <https://doi.org/10.3390/atmos11121376>
- Cheng, H., Edwards, R. L., Sinha, A., et al., 2016. The Asian Monsoon over the Past 640 000 Years and Ice Age Terminations. *Nature*, 534(7609): 640–646. <https://doi.org/10.1038/nature18591>
- D'Asaro, E. A., Black, P. G., Centurioni, L. R., et al., 2014. Impact of Typhoons on the Ocean in the Pacific. *Bulletin of the American Meteorological Society*, 95(9): 1405–1418. <https://doi.org/10.1175/bams-d-12-00104.1>

- Elsner, J. B., Liu, K. B., 2003. Examining the ENSO-Typhoon Hypothesis. *Climate Research*, 25: 43–54. <https://doi.org/10.3354/cr025043>
- Emanuel, K., 2005. Increasing Destructiveness of Tropical Cyclones over the Past 30 years. *Nature*, 436(7051): 686–688. <https://doi.org/10.1038/nature03906>
- Emile-Geay, J., Cane, M., Seager, R., et al., 2007. El Niño as a Mediator of the Solar Influence on Climate. *Paleoceanography*, 22(3): PA3210. <https://doi.org/10.1029/2006pa001304>
- Gao, S., Wang, D. D., Yang, Y., et al., 2016. Holocene Sedimentary Systems on a Broad Continental Shelf with Abundant River Input: Process-Product Relationships. *Geological Society, London, Special Publications*, 429(1): 223–259. <https://doi.org/10.1144/sp429.4>
- Goldsmith, S. T., Carey, A. E., Lyons, W. B., et al., 2008. Extreme Storm Events, Landscape Denudation, and Carbon Sequestration: Typhoon Mindulle, Choshui River, Taiwan. *Geology*, 36(6): 483–486. <https://doi.org/10.1130/g24624a.1>
- Grinsted, A., Moore, J. C., Jevrejeva, S., 2004. Application of the Cross Wavelet Transform and Wavelet Coherence to Geophysical Time Series. *Nonlinear Processes in Geophysics*, 11(5/6): 561–566. <https://doi.org/10.5194/npg-11-561-2004>
- Hale, R. P., Nittrouer, C. A., Liu, J. T., et al., 2012. Effects of a Major Typhoon on Sediment Accumulation in Fangliao Submarine Canyon, SW Taiwan. *Marine Geology*, 326/327/328: 116–130. <https://doi.org/10.1016/j.margeo.2012.07.008>
- He, Y. X., Zhou, X., Liu, Y., et al., 2014. Weakened Yellow Sea Warm Current over the Last 2–3 Centuries. *Quaternary International*, 349: 252–256. <https://doi.org/10.1016/j.quaint.2013.09.039>
- Henderson-Sellers, A., Zhang, H., Berz, G., et al., 1998. Tropical Cyclones and Global Climate Change: A Post-IPCC Assessment. *Bulletin of the American Meteorological Society*, 79(1): 19–38. [https://doi.org/10.1175/1520-0477\(1998\)079<0019:tcagcc>2.0.co;2](https://doi.org/10.1175/1520-0477(1998)079<0019:tcagcc>2.0.co;2)
- Howell, P., Pisiias, N., Ballance, J., et al., 2006. ARAND Time-Series Analysis Software. Brown University, Providence RI
- Hu, B. Q., Yang, Z. S., Zhao, M. X., et al., 2012. Grain Size Records Reveal Variability of the East Asian Winter Monsoon since the Middle Holocene in the Central Yellow Sea Mud Area, China. *Science China Earth Sciences*, 55(10): 1656–1668. <https://doi.org/10.1007/s11430-012-4447-7>
- Huang, E. Q., Tian, J., Qiao, P. J., et al., 2015. Early Interglacial Carbonate-Dilution Events in the South China Sea: Implications for Strengthened Typhoon Activities over Subtropical East Asia. *Quaternary Science Reviews*, 125: 61–77. <https://doi.org/10.1016/j.quascirev.2015.08.007>
- Huang, W. P., 2017. Modelling the Effects of Typhoons on Morphological Changes in the Estuary of Beinan, Taiwan. *Continental Shelf Research*, 135: 1–13. <https://doi.org/10.1016/j.csr.2017.01.011>
- Jian, Z. M., Wang, P. X., Saito, Y., et al., 2000. Holocene Variability of the Kuroshio Current in the Okinawa Trough, Northwestern Pacific Ocean. *Earth and Planetary Science Letters*, 184(1): 305–319. [https://doi.org/10.1016/s0012-821x\(00\)00321-6](https://doi.org/10.1016/s0012-821x(00)00321-6)
- Kang, N. Y., Kim, D., Elsner, J. B., 2019. The Contribution of Super Typhoons to Tropical Cyclone Activity in Response to ENSO. *Scientific Reports*, 9: 5046. <https://doi.org/10.1038/s41598-019-41561-y>
- Li, Y., Yu, H. J., Yi, L., et al., 2014. Grain-Size Characteristics and Its Sedimentary Significance of Coastal Sediments of the Borehole Lz908 in the South Bohai Sea (the Laizhou Bay), China. *Marine Sciences*, 38(5): 107–113. <https://doi.org/10.11759/hyxx20130120003> (in Chinese with English Abstract)
- Liang, C., Jiang, Z. X., Cao, Y. C., et al., 2017. Sedimentary Characteristics and Paleoenvironment of Shale in the Wufeng-Longmaxi Formation, North Guizhou Province, and Its Shale Gas Potential. *Journal of Earth Science*, 28(6): 1020–1031. <https://doi.org/10.1007/s12583-016-0932-x>
- Liu, G., Han, X. B., Chen, Y. P., et al., 2020. Magnetic Characteristics of Core YSC-10 Sediments in the Central Yellow Sea Mud Area and Implications for Provenance Changes. *Acta Sedimentologica Sinica*, 39(2): 383–394. <https://doi.org/10.14027/j.issn.1000-0550.2020.017> (in Chinese with English Abstract)
- Liu, J., Kong, X. H., Saito, Y., et al., 2013. Subaqueous Deltaic Formation of the Old Yellow River (AD 1128–1855) on the Western South Yellow Sea. *Marine Geology*, 344: 19–33. <https://doi.org/10.1016/j.margeo.2013.07.003>
- Liu, J. P., Milliman, J. D., Gao, S., et al., 2004. Holocene Development of the Yellow River's Subaqueous Delta, North Yellow Sea. *Marine Geology*, 209(1/2/3/4): 45–67. <https://doi.org/10.1016/j.margeo.2004.06.009>
- Liu, Z. J., Yu, J., Sun, X. Y., et al., 2016. A Discussion of Marine Sediments ¹⁴C Data Integration and Correction. *Quaternary Sciences*, 36(2): 492–502. <https://doi.org/10.11928/j.issn.1001-7410.2016.02.24> (in Chinese with English Abstract)
- Lyu, W. Z., Yang, J. C., Fu, T. F., et al., 2020. Asian Monsoon and Oceanic Circulation Paced Sedimentary Evolution over the Past 1 500 years in the Central Mud Area of the Bohai Sea, China. *Geological Journal*, 55(7): 5606–5618. <https://doi.org/10.1002/gj.3758>
- Ma, L. P., Chen, L. S., Xu, X. D., 2006. On the Characteristics of Correlation between Global Tropical Cyclone Activities and Global Climate Change. *Journal of Tropical Meteorology*, 22(2): 147–154. <https://doi.org/10.16032/j.issn.1004-4965.2006.02.006> (in Chinese with English Abstract)
- Manoj, M. C., Srivastava, J., Uddandam, P. R., et al., 2020. A 2 000 Year Multi-Proxy Evidence of Natural/Anthropogenic Influence on Climate from the Southwest Coast of India. *Journal of Earth Science*, 31(5): 1029–1044. <https://doi.org/10.1007/s12583-020-1336-4>
- McCloskey, T. A., Liu, K. B., 2012. A Sedimentary-Based History of Hurricane Strikes on the Southern Caribbean Coast of Nicaragua. *Quaternary Research*, 78(3): 454–464. <https://doi.org/10.1016/j.yqres.2012.07.003>
- McCloskey, T. A., Liu, K. B., 2013. A 7 000 Year Record of Paleohurricane Activity from a Coastal Wetland in Belize. *The Holocene*, 23(2): 278–291. <https://doi.org/10.1177/0959683612460782>
- Meehl, G. A., Arblaster, J. M., Matthes, K., et al., 2009. Amplifying the Pacific Climate System Response to a Small 11-Year Solar Cycle Forcing. *Science*, 325(5944): 1114–1118. <https://doi.org/10.1126/science.1172872>
- Mei, X., Li, R. H., Zhang, X. H., et al., 2016. Evolution of the Yellow Sea Warm Current and the Yellow Sea Cold Water Mass since the Middle Pleistocene. *Palaeogeography, Palaeoclimatology, Palaeoecology*, 442: 48–60. <https://doi.org/10.1016/j.palaeo.2015.11.018>
- Milliman, J. D., Lin, S. W., Kao, S. J., et al., 2007. Short-Term Changes in Seafloor Character Due to Flood-Derived Hyperpycnal Discharge: Typhoon Mindulle, Taiwan, July 2004. *Geology*, 35(9): 779–782. <https://doi.org/10.1130/g23760a.1>
- Misios, S., Gray, L. J., Knudsen, M. F., et al., 2019. Slowdown of the Walker Circulation at Solar Cycle Maximum. *Proceedings of the National Academy of Sciences of the United States of America*, 116(15): 7186–7191. <https://doi.org/10.1073/pnas.1815060116>
- Passaga, R., 1957. Texture as Characteristic of Clastic Deposition. *AAPG Bulletin*, 41(9): 1952–1984. <https://doi.org/10.1306/0bda594e-16bd-11d7-8645000102c1865d>
- Passaga, R., 1964. Grain Size Representation by CM Patterns as a Geologic Tool. *Journal of Sedimentary Research*, 34(4): 830–847. <https://doi.org/10.1306/0bda594e-16bd-11d7-8645000102c1865d>

- org/10.1306/74d711a4-2b21-11d7-8648000102c1865d
- Pausata, F. S. R., Camargo, S. J., 2019. Tropical Cyclone Activity Affected by Volcanically Induced ITCZ Shifts. *PNAS*, 116(16): 7732–7737. <https://doi.org/10.1073/pnas.1900777116>
- Peng, J., Luo, X. X., Liu, F., et al., 2018. Analysing the Influences of ENSO and PDO on Water Discharge from the Yangtze River into the Sea. *Hydrological Processes*, 32(8): 1090–1103. <https://doi.org/10.1002/hyp.11484>
- Qiao, S. Q., Shi, X. F., Wang, G. Q., et al., 2017. Sediment Accumulation and Budget in the Bohai Sea, Yellow Sea and East China Sea. *Marine Geology*, 390: 270–281. <https://doi.org/10.1016/j.margeo.2017.06.004>
- Reimer, P. J., Bard, E., Bayliss, A., et al., 2016. IntCal13 and Marine13 Radiocarbon Age Calibration Curves 0–50 000 Years cal BP. *Radiocarbon*, 55(4): 1869–1887. https://doi.org/10.2458/azu_js_rc.55.16947
- Ren, R., Chen, S. L., Dong, P., et al., 2012. Spatial and Temporal Variations in Grain Size of Surface Sediments in the Littoral Area of Yellow River Delta. *Journal of Coastal Research*, 278: 44–53. <https://doi.org/10.2112/jcoastres-d-11-00084.1>
- Shan, X., Shi, X. F., Clift, P. D., et al., 2019. Carbon Isotope and Rare Earth Element Composition of Late Quaternary Sediment Gravity Flow Deposits on the Mid Shelf of East China Sea: Implications for Provenance and Origin of Hybrid Event Beds. *Sedimentology*, 66(5): 1861–1895. <https://doi.org/10.1111/sed.12561>
- Shen, S. X., Chen, L. R., Gao, L., et al., 1993. Discovery of Holocene Cyclonic Eddy Sediment and Pathway Sediment in the Southern Yellow Sea. *Oceanologia et Limnologia Sinica*, 24(6): 563–570 (in Chinese with English Abstract)
- Siddall, M., Rohling, E. J., Almogi-Labin, A., et al., 2003. Sea-Level Fluctuations during the Last Glacial Cycle. *Nature*, 423(6942): 853–858. <https://doi.org/10.1038/nature01690>
- Steinhilber, F., Beer, J., Fröhlich, C., 2009. Total Solar Irradiance during the Holocene. *Geophysical Research Letters*, 36(19): L19704. <https://doi.org/10.1029/2009GL040142>
- Stuiver, M., Reimer, P. J., Reimer, R. W., 2019. CALIB 7.1. [2020-6-15]. <http://calib.org/calib/>
- Sun, J., Oey, L., Xu, F. H., et al., 2017. Sea Level Rise, Surface Warming, and the Weakened Buffering Ability of South China Sea to Strong Typhoons in Recent Decades. *Scientific Reports*, 7: 7418. <https://doi.org/10.1038/s41598-017-07572-3>
- Sun, X. G., Fang, M., Huang, W., 2000. Spatial and Temporal Variations in Suspended Particulate Matter Transport on the Yellow and East China Sea Shelf. *Oceanologia et Limnologia Sinica*, 31(6): 581–587. <https://doi.org/10.3321/j.issn:0029-814x.2000.06.001> (in Chinese with English Abstract)
- Tan, L., Cai, Y., An, Z., et al., 2011. Climate Patterns in North Central China during the Last 1 800 yr and Their Possible Driving Force. *Climate of the Past*, 7(3): 685–692. <https://doi.org/10.5194/cp-7-685-2011>
- Tang, Y. X., Zou, E. M., Lie, H. J., et al., 2000. Some Features of Circulation in the Southern Huanghai Sea. *Acta Oceanologica Sinica*, 22(1): 1–22. <https://doi.org/10.3321/j.issn:0253-4193.2000.01.001> (in Chinese with English Abstract)
- Tian, Y., Fan, D. J., Zhang, X. L., et al., 2019. Event Deposits of Intense Typhoons in the Muddy Wedge of the East China Sea over the Past 150 Years. *Marine Geology*, 410: 109–121. <https://doi.org/10.1016/j.margeo.2018.12.010>
- Tu, J. Y., Chou, C. A., Chu, P. S., 2009. The Abrupt Shift of Typhoon Activity in the Vicinity of Taiwan and Its Association with Western North Pacific-East Asian Climate Change. *Journal of Climate*, 22(13): 3617–3628. <https://doi.org/10.1175/2009jcli2411.1>
- Wada, A., Usui, N., 2007. Importance of Tropical Cyclone Heat Potential for Tropical Cyclone Intensity and Intensification in the Western North Pacific. *Journal of Oceanography*, 63(3): 427–447. <https://doi.org/10.1007/s10872-007-0039-0>
- Waelbroeck, C., Labeyrie, L., Michel, E., et al., 2002. Sea-Level and Deep Water Temperature Changes Derived from Benthic Foraminifera Isotopic Records. *Quaternary Science Reviews*, 21(1/2/3): 295–305. [https://doi.org/10.1016/s0277-3791\(01\)00101-9](https://doi.org/10.1016/s0277-3791(01)00101-9)
- Wang, F. F., Liu, J., Qiu, J. D., et al., 2014. Thickness variation and Provenance of Mid-Holocene Mud Sediments in the Central and Western South Yellow Sea. *Marine Geology & Quaternary Geology*, 34(5): 1–11. <https://doi.org/10.3724/sp.j.1140.2014.05001> (in Chinese with English Abstract)
- Wang, F. F., Yu, Z. G., Xu, B. C., et al., 2018. Nepartak Typhoon Influenced Bottom Sediments from the Yangtze River Estuary and Adjacent East China Sea-Foraminiferal Evidence. *Geochemistry, Geophysics, Geosystems*, 19(4): 1049–1063. <https://doi.org/10.1002/2017gc007413>
- Wang, L. C., Behling, H., Lee, T. Q., et al., 2014. Late Holocene Environmental Reconstructions and Their Implications on Flood Events, Typhoon, and Agricultural Activities in NE Taiwan. *Climate of the Past*, 10(5): 1857–1869. <https://doi.org/10.5194/cp-10-1857-2014>
- Wang, Y. J., Cheng, H., Edwards, R. L., et al., 2005. The Holocene Asian Monsoon: Links to Solar Changes and North Atlantic Climate. *Science*, 308(5723): 854–857. <https://doi.org/10.1126/science.1106296>
- Wang, Y. M., Ren, F. M., Li, W. J., et al., 2008. Climatic Characteristics of Typhoon Precipitation over China. *Journal of Tropical Meteorology*, 14(2): 125–128. <https://doi.org/10.16032/j.issn.1004-4965.2008.03.004>
- Webster, P. J., Holland, G. J., Curry, J. A., et al., 2005. Changes in Tropical Cyclone Number, Duration, and Intensity in a Warming Environment. *Science*, 309(5742): 1844–1846. <https://doi.org/10.1126/science.1116448>
- Woodruff, J. D., Donnelly, J. P., Okusu, A., 2009. Exploring Typhoon Variability over the Mid-to-Late Holocene: Evidence of Extreme Coastal Flooding from Kamikoshiki, Japan. *Quaternary Science Reviews*, 28(17/18): 1774–1785. <https://doi.org/10.1016/j.quascirev.2009.02.005>
- Yang, Z. S., Liu, J. P., 2007. A Unique Yellow River-Derived Distal Subaqueous Delta in the Yellow Sea. *Marine Geology*, 240(1/2/3/4): 169–176. <https://doi.org/10.1016/j.margeo.2007.02.008>
- Yao, H. Q., Wang, F. L., Wang, H. F., et al., 2021. Pleistocene Magnetostratigraphy of Four Cores in the West Philippian Basin and Regional Sedimentary Shift during the Mid-Pleistocene Transition. *Geological Journal*, 56(6): 2919–2929. <https://doi.org/10.1002/gj.4082>
- Ye Y. G., Wang X. E., Diao S. B., et al., 1989. Reports of ¹⁴C Dating (HD) I. *Marine Geology & Quaternary Geology*, 9(1): 115–120. <https://doi.org/10.16562/j.cnki.0256-1492.1989.01.016> (in Chinese with English Abstract)
- Yi, L., Chen, S. L., Ortiz, J. D., et al., 2016. 1 500-Year Cycle Dominated Holocene Dynamics of the Yellow River Delta, China. *The Holocene*, 26(2): 222–234. <https://doi.org/10.1177/0959683615596834>
- Yi, L., Shi, Z. G., Tan, L. C., et al., 2018. Orbital-Scale Nonlinear Response of East Asian Summer Monsoon to Its Potential Driving Forces in the Late Quaternary. *Climate Dynamics*, 50(5/6): 2183–2197. <https://doi.org/10.1007/s00382-017-3743-5>
- Ying, M., Zhang, W., Yu, H., et al., 2014. An Overview of the China Meteorological Administration Tropical Cyclone Database. *Journal of Atmospheric and Oceanic Technology*, 31(2): 287–301. <https://doi.org/10.1175/jtech-d-12-00119.1>

- Zhang, K. D., Li, A. C., Zhang, J., et al., 2018. Recent Sedimentary Records in the East China Sea Inner Shelf and Their Response to Environmental Change and Human Activities. *Journal of Oceanology and Limnology*, 36(5): 1537–1555. <https://doi.org/10.1007/s00343-018-7028-6>
- Zhang, L., Chen, S. L., Pan, S. Q., et al., 2014. Sediment Variability and Transport in the Littoral Area of the Abandoned Yellow River Delta, Northern Jiangsu. *Journal of Geographical Sciences*, 24(4): 717–730. <https://doi.org/10.1007/s11442-014-1115-1>
- Zhang, Y. F., Hu, C. L., Wang, X. M., et al., 2017. An Improved Method of Laser Particle Size Analysis and Its Applications in Identification of Lacustrine Tempestite and Beach Bar: An Example from the Dongying Depression. *Journal of Earth Science*, 28(6): 1145–1152. <https://doi.org/10.1007/s12583-016-0930-1>
- Zhang, Y. C., Zhou, X., He, Y. X., et al., 2019. Persistent Intensification of the Kuroshio Current during Late Holocene Cool Intervals. *Earth and Planetary Science Letters*, 506: 15 – 22. <https://doi.org/10.1016/j.epsl.2018.10.018>
- Zhou, L., Gao, S., Yang, Y., et al., 2017. Typhoon Events Recorded in Coastal Lagoon Deposits, Southeastern Hainan Island. *Acta Oceanologica Sinica*, 36(4): 37–45. <https://doi.org/10.1007/s13131-016-0918-6>
- Zhou, L., Yang, Y., Wang, Z. H., et al., 2019. Investigating ENSO and WPWP Modulated Typhoon Variability in the South China Sea during the Mid–Late Holocene Using Sedimentological Evidence from Southeastern Hainan Island, China. *Marine Geology*, 416: 105987. <https://doi.org/10.1016/j.margeo.2019.105987>
- Zhou, X., Liu, Z. H., Yan, Q., et al., 2019. Enhanced Tropical Cyclone Intensity in the Western North Pacific during Warm Periods over the Last Two Millennia. *Geophysical Research Letters*, 46(15): 9145 – 9153. <https://doi.org/10.1029/2019gl083504>
- Zhou, X., Sun, L. G., Huang, W., et al., 2014. Relationship between Magnetic Susceptibility and Grain Size of Sediments in the China Seas and Its Implications. *Continental Shelf Research*, 72: 131–137. <https://doi.org/10.1016/j.csr.2013.07.011>
- Zou, E. M., Guo, B. H., Tang, Y. X., et al., 2001. An Analysis of Summer Hydrographic Features and Circulation in the Southern Yellow Sea and the Northern East China Sea. *Oceanologia et Limnologia Sinica*, 32(3): 340–348 (in Chinese with English Abstract)